

## Unraveling the self-assembly modes in multi-component supramolecular gels using single crystal X-ray diffraction

Dipankar Ghosh, Abbas D. Farahani, Adam D Martin, Pall Thordarson, and Krishna K. Damodaran

*Chem. Mater.*, **Just Accepted Manuscript** • DOI: 10.1021/acs.chemmater.0c00475 • Publication Date (Web): 01 Apr 2020

Downloaded from [pubs.acs.org](https://pubs.acs.org) on April 6, 2020

### Just Accepted

“Just Accepted” manuscripts have been peer-reviewed and accepted for publication. They are posted online prior to technical editing, formatting for publication and author proofing. The American Chemical Society provides “Just Accepted” as a service to the research community to expedite the dissemination of scientific material as soon as possible after acceptance. “Just Accepted” manuscripts appear in full in PDF format accompanied by an HTML abstract. “Just Accepted” manuscripts have been fully peer reviewed, but should not be considered the official version of record. They are citable by the Digital Object Identifier (DOI®). “Just Accepted” is an optional service offered to authors. Therefore, the “Just Accepted” Web site may not include all articles that will be published in the journal. After a manuscript is technically edited and formatted, it will be removed from the “Just Accepted” Web site and published as an ASAP article. Note that technical editing may introduce minor changes to the manuscript text and/or graphics which could affect content, and all legal disclaimers and ethical guidelines that apply to the journal pertain. ACS cannot be held responsible for errors or consequences arising from the use of information contained in these “Just Accepted” manuscripts.

# Unraveling the self-assembly modes in multi-component supramolecular gels using single crystal X-ray diffraction.

Dipankar Ghosh,<sup>†</sup> Abbas D. Farahani,<sup>‡</sup> Adam D. Martin,<sup>§</sup> Pall Thordarson,<sup>\* ‡</sup> and Krishna K. Damodaran<sup>\* †</sup>

<sup>†</sup>Department of Chemistry, Science Institute, University of Iceland, Dunhagi 3, 107 Reykjavík, Iceland. Tel: +354 525 4846, Fax: +354 552 8911.

<sup>‡</sup>School of Chemistry, The Australian Centre for Nanomedicine and the ARC Centre of Excellence in Convergent Bio-Nano Science and Technology, University of New South Wales, Sydney-2052, Australia

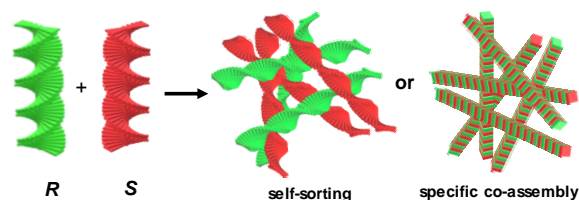
<sup>§</sup>Dementia Research Centre, Department of Biomedical Science, Faculty of Medicine and Health Sciences, Macquarie University, Sydney, NSW 2109, Australia

**ABSTRACT:** The control and prediction of the self-assembly process in multi-component supramolecular gels is challenging because the structure and properties rely mostly on the geometry and spatial arrangement of the building blocks. The understanding of non-covalent interactions between the individual gelators at molecular level will enable us to tune the gelation properties of multi-component gels. We have studied the self-assembly process of multi-component gel based on enantiomers and report the first crystallographic evidence of specific co-assembly in mixed enantiomeric gel, which is supported by scanning electron microscopy (SEM) and atomic force microscopy (AFM) images. The mode of interactions between the individual gelators from molecular to macroscopic level, which are responsible for co-assembled fibers was identified by single crystal X-ray diffraction. We have proved that specific co-assembly leads to enhanced mechanical and thermal stability in the mixed gel compared to the meso and individual enantiomeric gels.

## INTRODUCTION

Self-assembly is an ubiquitous process in life science and nature has been successful in self-assembling simple building blocks to complex functional architectures with unique functions and properties.<sup>1</sup> The concept of supramolecular chemistry<sup>2,3</sup> has enabled chemists to mimic nature's self-assembly principles resulting in functional materials with tailored properties<sup>4-6</sup> but it is often challenging to control the structure and mechanism of such self-assembled structures and their formation in real-time. Stimuli-responsive supramolecular systems<sup>7-10</sup> offer better control of the self-assembly/reassembly process, which can be either switched on/off by an external stimulus such as anions, heat, light, sound etc. Supramolecular low molecular weight gelators (LMWGs)<sup>11-19</sup> based on multi-component systems have emerged as an important class of stimuli-responsive soft materials due to their potential applications in tuning gel state properties.<sup>20-25</sup> Multi-component gels obtained by mixing individual gels offer a good platform to analyze the supramolecular assembly of individual gels. For example, the individual gelator molecules interact either constructively or destructively to form well-ordered fibers containing individual gelators (self-sorting), both gelators (specific co-assembly, Scheme 1) or a mixture of both (random co-assembly).<sup>24, 25</sup> Multi-component self-assembled gels obtained by mixing enantiomers<sup>25-37</sup> display interesting properties due to the interaction between pure enantiomers, which facilitates the formation of mixed enantiomeric gels

with intriguing properties that are not achieved by individual enantiomeric gels. These interactions will lead to more favorable packing in mixed enantiomeric gels,<sup>25-37</sup> presumably due to the interaction of the individual enantiomers either constructively or destructively. Recently, we have shown that mixing enantiomeric bis(urea) compounds tagged with a phenylalanine methyl ester led to a multi-component gel with enhanced thermal and mechanical strength.<sup>30</sup>



**Scheme 1:** Self-sorting and specific co-assembly of enantiomers in mixed gels.

One of the main challenges in mixed gel systems is the prediction of the self-assembly process, because it is hard to control the interactions between the individual gelators from molecular to macroscopic level during the formation of fibrous networks.<sup>25, 38, 39</sup> The self-assembly process at the molecular level in multi-component gels have been analyzed by various spectroscopic<sup>40-46</sup> and microscopic techniques.<sup>47-51</sup> Efforts have been made to unravel the self-assembly process of multi-component enantiomeric gels by analyzing the physical properties using spectroscopic

methods such as UV-vis, NMR and IR and other methods such as differential scanning calorimetry (DSC) and rheology.<sup>52-59</sup> We have studied the self-assembly process in mixed enantiomeric gels using SEM, AFM and solid-state NMR and showed that the resulting network is a mixture of self-sorted and co-assembled networks.<sup>30</sup> Recent developments in high-resolution X-ray diffraction has enabled researchers to differentiate self-sorted and co-assembled networks and identify the key parameters in the formation of multi-component gel networks.<sup>24, 48, 59-63</sup> Adams and co-workers used fiber X-ray diffraction to show self-sorting in naphthalene-functionalized dipeptide hydrogelators.<sup>59</sup> Nisbet *et al* showed that the small angle X-ray scattering (SAXS) data of co-assembled system was different from the individual components.<sup>60</sup> Adams *et al* proved that the individual components in multi-component dipeptides gels are self-sorted by isolating the single crystals of one the dipeptides in the gel network.<sup>24</sup>

Single crystal X-ray diffraction (SCXRD) has been used to identify the key interactions in the solid-state structure of LMWGs,<sup>64-71</sup> which may provide some insight into the packing modes of these molecules in gel fibers. This approach was used by Pfeffer and co-workers to explain the gelation behavior of the enantiomers compared to the non-gelator racemate.<sup>72</sup> However, the analysis of the self-assembly process in multi-component gels based on enantiomers using single crystal X-ray diffraction is not reported till date due to the lack of crystal structures of all possible stereoisomeric forms and the mixed enantiomers. The combination of single crystal X-ray structure of the gelator and powder diffraction pattern of either the native gel or the xerogel will enable us to correlate the intermolecular interactions observed in the single crystal structure with the molecular aggregation in the gel state. Although, the removal of solvent to prepare a xerogel can result in artefacts due to dissolution, recrystallisation and changes in morphology or polymorphic phase transition, but this approach still remains as one of the practical methods to get insight to self-assembly process in LMWGs.<sup>12, 19, 71, 73, 74</sup> Interestingly, this approach has not been explored for enantiomeric multi-component gels due to the high scattering factor of the gel systems and also the non-availability of the structural information for comparison. In this work, we have used X-ray diffraction to correlate the solid-state structures of multi-component gel based on bis-amides of terephthalic acid and amino acid derivatives with the dried gel state. To the best of our knowledge, this is the first example correlating the self-assembly process of the gelator with its crystal structure in multi-component gels based on enantiomers.

## EXPERIMENTAL SECTION

### Materials and methods

All the starting materials and reagents were commercially available (Sigma Aldrich and TCI Europe) and used as supplied. Enantiomeric (*S* or *R*)-methyl valinate was purchased as hydrochloride salt and the racemate in acid form. Deionized water and freshly distilled ethanol were used for gelation and CD experiments. Dichloromethane (DCM) was distilled over CaH<sub>2</sub> prior to use in synthesis. Methyl *rac*-valinate was synthesized following similar reported procedure.<sup>75</sup> **SS-TAV** is reported,<sup>76</sup> **RR-TAV** and **TAV** were

synthesized in similar fashion. The mono *tert*-butyl ester of terephthalic acid (**1**) was synthesized according to the literature.<sup>77</sup> <sup>1</sup>H and <sup>13</sup>C NMR spectra were recorded on a Bruker Advance 400 spectrometer. ATR-FTIR and CD was measured in a Nicolet iZ10 and a Jasco J-1100 CD spectrometer respectively. SEM and AFM were performed on a Leo Supra 25 microscope and a Bruker MultiMode 8 respectively. Single crystal X-ray diffraction (SCXRD) and PXRD was carried out using a Bruker D8 venture and Bruker D8 Focus instrument. High-Performance Liquid Chromatography (HPLC) was performed on a Shimadzu Prominence LC-20A HPLC system to confirm purity of the compounds.

### Synthesis

**Methyl *rac*-valinate:** *rac*-valine (3.0 g, 25.6 mmol) was dissolved in 50 mL of methanol and 4 mL (6.5 g, 55.0 mmol) of thionyl chloride was added dropwise. The solution was refluxed at 65 °C for 8 hours and then cooled to room temperature. Methanol was evaporated and the white oil obtained was stirred with 2% NaHCO<sub>3</sub> solution. The solution was extracted with dichloromethane (3 × 50 mL), the combined organic layers were dried over Na<sub>2</sub>SO<sub>4</sub> and evaporated to yield the ester as colorless oil. Yield: 2.6 g, 77%. <sup>1</sup>H NMR (400 MHz, CDCl<sub>3</sub>): δ [ppm] = 3.71 (3H, s), 3.29 (1H, d, J = 5.2), 2.01 (1H, m), 1.42 (2H, bs), 0.96 (3H, d, J = 6.8), 0.90 (3H, d, J = 6.8). <sup>13</sup>C NMR (100 MHz, CDCl<sub>3</sub>): δ [ppm] = 176.10, 60.08, 51.82, 32.32, 19.40, 17.32.

**SS-TAV and RR-TAV:** Terephthaloyl dichloride (1.0 g, 4.9 mmol) and corresponding (*S* or *R*)-methyl valinate hydrochloride (1.7 g, 10.0 mmol) were taken in 2-neck RB flask under dry N<sub>2</sub> atmosphere at 0 °C, and 40 mL freshly distilled DCM was added to it. A solution of 3 mL (2.1 g, 21.5 mmol) triethylamine in 30 mL dry DCM was added dropwise to the above solution, and the mixture was stirred overnight at room temperature. The clear solution was washed with 3.0% NaHCO<sub>3</sub>, 0.05 N HCl followed by brine. The organic layer was dried over Na<sub>2</sub>SO<sub>4</sub> and evaporated to yield the desired amide as white solid.

**SS-TAV:** Yield 1.9 g, 98.5%. <sup>1</sup>H NMR (400 MHz, CDCl<sub>3</sub>): δ [ppm] = 7.87 (4H, s), 6.67 (2H, d, J = 8.4), 4.78 (2H, dd, J = 8.8, 5.0), 3.79 (6H, s), 2.29 (2H, m), 1.02 (6H, d, J = 6.8), 1.00 (6H, d, J = 7.2). <sup>13</sup>C NMR (100 MHz, CDCl<sub>3</sub>): δ [ppm] = 172.50, 166.30, 137.00, 127.40, 57.56, 52.33, 31.63, 18.99, 18.00. HRMS (APCI) calculated for C<sub>20</sub>H<sub>28</sub>N<sub>2</sub>O<sub>6</sub>Na [M+Na]<sup>+</sup> 415.1840; found 415.1831.

**RR-TAV:** Yield 1.88 g, 97.5%. <sup>1</sup>H NMR (400 MHz, CDCl<sub>3</sub>): δ [ppm] = 7.87 (4H, s), 6.69 (2H, d, J = 8.4), 4.78 (2H, dd, J = 8.8, 5.0), 3.78 (6H, s), 2.29 (2H, m), 1.02 (6H, d, J = 6.8), 1.00 (6H, d, J = 7.2). <sup>13</sup>C NMR (100 MHz, CDCl<sub>3</sub>): δ [ppm] = 172.47, 166.30, 136.98, 127.39, 57.55, 52.32, 31.62, 18.99, 18.00. HRMS (APCI) calculated for C<sub>20</sub>H<sub>28</sub>N<sub>2</sub>O<sub>6</sub>Na [M+Na]<sup>+</sup> 415.1840; found 415.1828.

**TAV:** The ternary mixture consisting of racemate and meso form (**TAV**) was synthesized in similar procedure except *rac*-methyl valinate (1.3 g, 10.0 mmol) was used in amine form and 1.5 mL (1.1 g, 11.0 mmol) triethylamine was added during the reaction. Yield: 1.89 g, 98.0%. <sup>1</sup>H NMR (400 MHz, CDCl<sub>3</sub>): δ [ppm] = 7.86 (4H, s), 6.75 (2H, d, J = 8.4), 4.77 (2H, dd, J = 8.8, 5.0), 3.77 (6H, s), 2.28 (2H, m), 1.01 (6H, d, J = 7.2), 0.99 (6H, d, J = 6.8). <sup>13</sup>C NMR (100 MHz,

CDCl<sub>3</sub>):  $\delta$  [ppm] = 172.51, 166.51, 137.02, 127.56, 57.70, 52.45, 31.71, 19.12, 18.15. HRMS (APCI) calculated for C<sub>20</sub>H<sub>28</sub>N<sub>2</sub>O<sub>6</sub>Na [M+Na]<sup>+</sup> 415.1840; found 415.1829.

**tert-butyl (S)-4-((1-methoxy-3-methyl-1-oxobutan-2-yl)-carbamoyl)benzoate (2):** 4-(tert-butoxycarbonyl)benzoic acid (**1**)<sup>77</sup> (2.2 g, 10 mmol), 3 mL (4.9 g, 41.3 mmol) of thionyl chloride and 5 mL dry DCM was stirred at in a RB flask under nitrogen at 45.0 °C overnight. The clear solution obtained was evaporated under reduced pressure to remove the volatile impurities leaving tert-butyl-4-(chlorocarbonyl)benzoate as white solid and 50 mL dry DCM was added. Methyl S-valinate hydrochloride (1.7 g, 10.0 mmol) was added to this mixture and was cooled to at 0 °C under N<sub>2</sub> atmosphere followed by the dropwise addition of a solution of 3.5 mL (2.5 g, 25.1 mmol) triethylamine in 50 mL dry DCM. The mixture was stirred overnight at room temperature, then washed with 3.0% NaHCO<sub>3</sub>, 0.05 N HCl and brine. The organic layer was dried over Na<sub>2</sub>SO<sub>4</sub> and evaporated to yield the mono-amide mono-tert-butyl ester (**2**) as pale yellow solid. Yield 2.7 g, 80.6%. <sup>1</sup>H NMR (400 MHz, CDCl<sub>3</sub>):  $\delta$  [ppm] = 8.04 (2H, d, J = 8.8), 7.83 (2H, d, J = 8.4), 6.68 (1H, d, J = 8.4), 4.78 (1H, dd, J = 8.6, 5.0), 3.78 (3H, s), 2.28 (1H, m), 1.60 (9H, s), 1.01 (3H, d, J = 6.8), 0.99 (3H, d, J = 7.2). <sup>13</sup>C NMR (100 MHz, CDCl<sub>3</sub>):  $\delta$  [ppm] = 172.50, 166.52, 164.82, 137.48, 134.85, 129.66, 126.90, 81.67, 57.54, 52.33, 31.65, 28.13, 18.99, 18.01. HRMS (APCI) calculated for C<sub>18</sub>H<sub>25</sub>NO<sub>5</sub>Na [M+Na]<sup>+</sup> 358.1625; found 358.1615.

**(S)-4-((1-methoxy-3-methyl-1-oxobutan-2-yl)carbamoyl)-benzoic acid (3):** To a solution of **2** (2.7 g, 8.0 mmol) in 16 mL DCM, 8 mL (11.9 g, 10.4 mmol) of trifluoroacetic acid (TFA) was added. The reaction mixture was stirred overnight at room temperature, volatile impurities were evaporated, and the residue was passed through a column (silica gel, DCM/MeOH 4:1). The product was obtained as white solid. Yield 2.1 g, 93.8%. <sup>1</sup>H NMR (400 MHz, CDCl<sub>3</sub>):  $\delta$  [ppm] = <sup>1</sup>H NMR (400 MHz, CDCl<sub>3</sub>):  $\delta$  [ppm] = 10.12 (1H, bs), 8.07 (2H, d, J = 8.4), 7.84 (2H, d, J = 8.8), 6.99 (1H, d, J = 8.8), 4.78 (1H, dd, J = 8.8, 5.2), 3.78 (3H, s), 2.30 (1H, m), 1.02 (3H, d, J = 6.8), 1.00 (3H, d, J = 6.4). <sup>13</sup>C NMR (100 MHz, CDCl<sub>3</sub>):  $\delta$  [ppm] = 173.02, 169.74, 166.93, 138.41, 132.16, 130.31, 127.20, 57.70, 52.46, 31.41, 18.98, 17.99. HRMS (APCI) calculated for C<sub>14</sub>H<sub>17</sub>NO<sub>5</sub>Na [M+Na]<sup>+</sup> 302.0999; found 302.1000.

**RS-TAV (4):** To a suspension of mono carboxylic acid **3** (2.1 g, 7.5 mmol) in 5 mL dry DCM, 2.2 mL (3.6 g, 30.3 mmol) of thionyl chloride was added under N<sub>2</sub> atmosphere and the reaction mixture was stirred at 45.0 °C overnight. A clear solution was observed, and the solvents were removed to yield the acid chloride methyl (4-(chlorocarbonyl)benzoyl)-S-valinate as white solid powder. 50 mL dry DCM was charged to the acid chloride and methyl R-valinate hydrochloride (1.3 g, 7.5 mmol) was subsequently added to a mixture under N<sub>2</sub> atmosphere. A solution of 2.6 mL (1.9 g, 18.7 mmol) triethylamine in 50 mL dry DCM was added dropwise to the mixture at 0 °C and stirred overnight at room temperature. The solution was washed with 3.0% NaHCO<sub>3</sub>, 0.05 N HCl and brine. The organic layer was dried over Na<sub>2</sub>SO<sub>4</sub> and evaporated to yield **RS-TAV** as pale brown solid. Yield 2.7 g, 93.3%. The purity of the meso compound was confirmed by chiral HPLC (see Supporting Information, Figure S22) <sup>1</sup>H NMR (400 MHz, CDCl<sub>3</sub>):  $\delta$  [ppm] = 7.87 (4H, s),

6.68 (2H, d, J = 8.8), 4.78 (2H, dd, J = 8.4, 4.8), 3.79 (6H, s), 2.29 (2H, m), 1.02 (6H, d, J = 7.2), 1.00 (6H, d, J = 7.2). <sup>13</sup>C NMR (100 MHz, CDCl<sub>3</sub>):  $\delta$  [ppm] = 172.46, 166.29, 136.99, 127.38, 57.55, 52.43, 31.63, 18.91, 17.99. HRMS (APCI) calculated for C<sub>20</sub>H<sub>28</sub>N<sub>2</sub>O<sub>6</sub>Na [M+Na]<sup>+</sup> 415.1840; found 415.1834.

#### Gelation Details

**Gelation test:** The required amount of the gelator was taken in a standard 7.0 mL vial, and 1.0 mL of appropriate solvent was added. The (**RR+SS**)-**TAV** gel was prepared by mixing equimolar ratio of individual **RR-TAV** and **SS-TAV** compounds, followed by the addition of the solvent/solvent mixture. The vial was closed, and the mixture was heated until a clear solution was observed. The solution was left undisturbed for gelation and gel formation was confirmed by inversion test.

**Minimum Gel Concentration (MGC):** Various amount of the gelator was weighted and gelation experiment was carried out as described above. The minimum amount of the gelator required to form gel after 24 hours was noted as minimum gel concentration (MGC).

**T<sub>gel</sub> Experiment:** 40.0 mg of the gelator was taken in a standard 7.0 mL vial and 1.0 mL of appropriate solvent was added. The mixture was heated to form a clear solution and kept undisturbed. After 24 h, a small spherical glass ball (54.0 mg) was carefully placed on the top of the gel. The vial was immersed in an oil bath equipped with a magnetic stirrer and a thermosensor. Temperature of the oil bath was gradually increased by ~10 °C per minute. The temperature at which the glass ball touched the bottom of the vial was recorded as T<sub>gel</sub>.

**Rheology:** Rheological measurements for *m*-xylene gels were carried out using MCR 102 Anton Paar modular compact rheometer using a 25.0 mm stainless steel parallel plate geometry configuration. The gels **RR-TAV**, **SS-TAV** and **RS-TAV** were prepared by dissolving 80.0 mg of corresponding gelator in 2.0 mL of *m*-xylene. The (**RR+SS**)-**TAV** gel was prepared by dissolving a mixture of 40.0 mg **RR-TAV** and 40.0 mg **SS-TAV** in 2.0 mL of *m*-xylene. Experiments were performed by scoping a ~2.0 mL portion of gel on the plate. Viscoelastic properties were evaluated by oscillatory measurements at a constant temperature of 25.0 °C. Amplitude sweeps were performed with constant frequency (*f*) of 1.0 Hz and log ramp strain ( $\gamma$ ) = 0.01 – 100% and frequency sweeps were carried out between 0.1 and 10.0 Hz within the linear viscoelasticity domain (0.1% strain). Rheology measurements for EtOH/water gels were made on an Anton Paar MCR 302 rheometer using a 25 mm stainless steel parallel plate geometry configuration and analyzed using the RheoCompass 1.24 software. Typical rheology measurements involved casting the sol (550  $\mu$ L, 4.0 wt% in EtOH: H<sub>2</sub>O (1:1, v/v)) onto one of the stainless-steel plates, lowering the other plate to the measurement position (1 mm) and for most of the cases the gels were formed in 3 hours. Then gels were allowed to form followed by applying constant frequency (*f*) = 1 Hz and strain ( $\gamma$ ) = 0.2% until a plateau in the storage modulus was observed. To avoid evaporation and maintain a temperature of 25.0 °C for frequency and amplitude sweeps, we used a Peltier temperature control hood. Frequency sweeps were undertaken 3

times with a log ramp frequency ( $f$ ) = 0.01 – 10 Hz in constant strain ( $\gamma$ ) = 0.2%. Amplitude sweeps were also performed with constant frequency ( $f$ ) = 1 Hz and log ramp strain ( $\gamma$ ) = 0.1 – 100%.

**Scanning Electron Microscopy (SEM):** All gels were prepared at 4.0 wt% and filtered after 24 h. The residue was dried in air and a small portion of the xerogel was placed on a pin mount with carbon tab on top and was coated with gold for three minutes. Morphologies of the dried gels were examined on a Leo Supra 25 microscope with in-lens detector at an operating voltage of 3 kV, with a working distance between 3 to 4 mm.

**Atomic Force Microscopy (AFM):** Solutions were prepared at 0.25 wt% in a 1:1 EtOH/water (v/v) mixture and cast onto a freshly cleaved mica substrate, followed by spreading of the drop over the mica using a glass slide, with the excess liquid wicked away using capillary action. These samples were left to dry in air overnight. Imaging was undertaken on a Bruker Multimode 8 atomic force microscope in ScanAsyst mode in air, whereby the imaging parameters are constantly optimized through the force curves that are collected, preventing damage of soft samples. Bruker ScanAsyst-Air probes were used, with a spring constant of 0.4 – 0.8 N/m and a tip radius of 2 nm.

**Circular Dichroism (CD):** The data were collected using a Jasco J-1100 CD spectrometer between wavelengths of 190 and 350 nm at 20 nm per minute rate, bandwidth of 1 nm and continues scanning mode. All gels were prepared at 5.0 wt% in EtOH/water (1:1 v/v). After 24 h, the gels were dispersed in EtOH/water (1:1 v/v) to obtain various concentrations (0.025, 0.03 and 0.05 wt%) and 0.03 wt% was found to be the optimum concentration. CD experiments in solution state were performed by dissolving 10.0 mg of the gelator in 3.0 mL of absolute EtOH and diluting 10 times in the same solvent.

### Crystallography

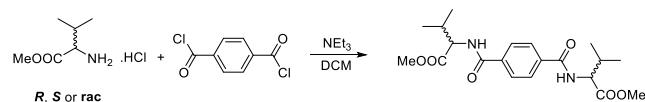
**Single-crystal X-ray Diffraction (SCXRD):** The compound (approximately 30.0 mg) was dissolved in 2.0 mL of suitable solvent and left in an open vial for crystallization. X-ray quality single crystals were isolated from mother liquor and quickly immersed in cryogenic oil and then mounted. The diffractions were collected using  $\text{CuK}\alpha$  radiation ( $\lambda = 1.542 \text{ \AA}$ ) on a Bruker D8 Venture (Photon100 CMOS detector) diffractometer equipped with a Cryostream (Oxford Cryosystems) open-flow nitrogen cryostats at a temperature of 120(2) K for the meso compound and all other compounds were collected at 150(2) K. The unit cell determination, data collection, data reduction, structure solution/refinement and empirical absorption correction (SADABS) were carried out using Apex-III (Bruker AXS: Madison, WI, 2015). All structure was solved by direct method and refined by the full-matrix least squares on  $F^2$  for all data using OLEX2<sup>78</sup> and SHELXTL<sup>79</sup> software. All non-disordered non-hydrogen atoms were refined anisotropically except for both the enantiomers. In these cases, the aromatic carbon atoms and the methoxy carbon atom of ester moieties were disordered and the free variables were refined by FVAR instruction. All the hydrogen atoms were placed in the calculated positions and refined using a riding model. Crystallographic data for the structures have been deposited to Cambridge

Crystallographic Data Centre as supplementary publication (CCDC no: 1975764-1975767).

**Powder X-ray Diffraction (PXRD):** The bulk compounds as synthesized were grinded to make a fine powder, and PXRD was performed on a Bruker D8 Focus instrument between  $2\theta$  value of 4.0 to 60.0. PXRD was also performed on the xerogels obtained similar way for SEM analysis.

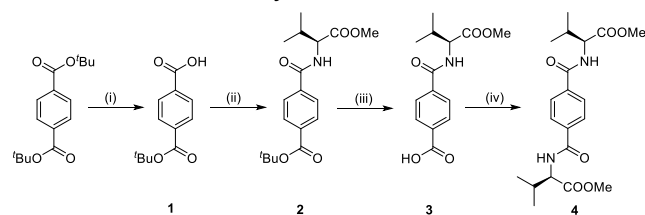
## RESULTS AND DISCUSSION

The chiral and achiral bis-amide compounds such as enantiomeric and meso forms were synthesized and characterized using standard analytical techniques including single crystal X-ray diffraction (SCXRD). Chiral LMWGs have emerged as a special class of soft materials due to their potential applications in chiral nanomaterials, chiral recognition and asymmetric catalysis.<sup>28, 47, 80-82</sup> The molecular chirality of a particular enantiomer is often translated into gel fibres.<sup>36, 83</sup> We have selected terephthalic amide of an amino acid ester (methyl valinate) owing to their ability to form  $C_2$ -symmetric chiral LMWGs.<sup>84-90</sup>



**Scheme 2:** Synthesis of *RR*-TAV, *SS*-TAV and TAV.

The terephthalic amide of amino acid ester is an ideal candidate for multi-component gels based on enantiomers due to their availability in both enantiomeric and racemic forms, inexpensive starting materials, crystalline nature and ease of modification.<sup>91, 92</sup> The hydrogen bonding interactions between the amide groups and  $\pi$ - $\pi$  interaction of the phenylene ring play an important role in the self-assembly process.<sup>87-90</sup> The diamides will display  $\beta$ -tape type self-assembly to form a well-defined fibrous network resulting in the formation of various organo/hydrogels similar to the self-assembly process in peptides. The self-assembly mode of the amide group is preserved by introducing the ester derivatives, which will interfere the hydrogen bonding between amide and carboxylate functionalities.<sup>93</sup>



**Scheme 3:** Synthesis of *RS*-TAV; (i) KOH &  $t\text{BuOH}$ , (ii)  $\text{SOCl}_2$ , *S*-methyl valinate hydrochloride,  $\text{Et}_3\text{N}$  and DCM, (iii) TFA & DCM and (iv)  $\text{SOCl}_2$ , *R*-methyl valinate hydrochloride,  $\text{Et}_3\text{N}$  and DCM.

Thus, we have synthesized enantiopure *R-R*-, *S-S*- and *R-S*-TAV based upon the valine methyl ester and terephthalic acid. Enantiopure *RR*-TAV and *SS*-TAV compounds were synthesized by reacting terephthaloyl dichloride and the corresponding *R*- or *S*-methyl valinate hydrochloride in dichloromethane (Scheme 2) in presence of triethylamine ( $\text{Et}_3\text{N}$ ). The meso form *RS*-TAV with *R-S* configuration was synthesized by reacting mono ester protected terephthalic acid chloride and *S*-methyl valinate hydrochloride to form a mono ester terephthalic amide with *S*-configuration, which was hydrolyzed, converted to acid chloride and reacted

with *R*-methyl valinate hydrochloride to form **RS-TAV** (Scheme 3). We have also synthesized **TAV** for comparison from terephthaloyl dichloride and racemate methyl valinate, which is expected to be a 1:1:2 mixture of *R-R*, *S-S* and *R-S* isomers. The compounds were characterized by NMR, IR, mass spectroscopy and single crystal X-ray diffraction (SCXRD). The chirality of the compounds was confirmed by circular dichroism (CD) experiments and the gelation properties were analyzed in a series of solvents using standard gelation techniques.

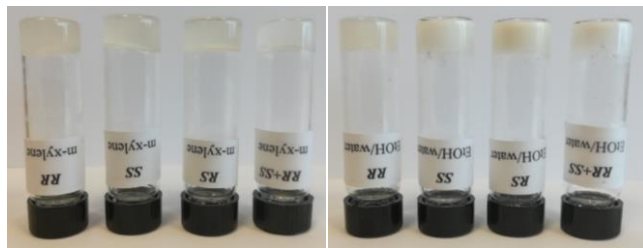


**Figure 1:** Gels obtained from **TAV** gelators- (left) in *m*-xylene and (right) in EtOH/water (1:1 v/v).

The gelation test was carried out by heating the gelator and the particular solvent in a sealed vial until a clear solution was obtained. The solution was sonicated prior to cooling in some cases to induce gelation, left undisturbed and the gel formation was confirmed by a vial inversion test (Figure 1). Gelation was mostly observed in aromatic solvents for all compounds (see Supporting Information, Table S1) such as benzene, toluene, *o*-xylene, *m*-xylene, *p*-xylene, and mesitylene, which may be attributed to the  $\pi$ - $\pi$  interactions between the phenylene rings of the gelator and the aromatic solvents. In chlorobenzene, the *meso* compound (**RS-TAV**) did not form a gel but the enantiopure **RR-TAV** and **SS-TAV** formed a gel at 5.5 wt% (wt% refers to w/v% in all cases). Interestingly, gelation was not observed in various aliphatic solvents (<6.0 wt%) such as DCM, chloroform, 1,2-dichloroethane, acetone, butanone, THF, 1,4-dioxane, acetonitrile, methanol, ethanol, isopropanol and butanol. The higher solubility of the gelator in these solvents may be attributed to the presence of strong hydrogen bonding motifs or polar moieties, which hinders  $\beta$ -tape formation. The compounds were unable to form hydrogels due to their insolubility in water. This prompted us to check the gelation properties of these compounds in mixed solvent systems (1:1, v/v) by dissolving the compound in polar solvents (either methanol, ethanol, isopropanol and *tert*-butanol) followed by the addition of water. The resulting aqueous solutions were heated, cooled and left undisturbed, and gels were formed in all cases (see Supporting Information, Table S2).

The minimum gel concentration (MGC) of the gelators were evaluated in benzene, toluene, *o*-xylene, *m*-xylene, *p*-xylene and mesitylene (Table 1). The MGC for *meso* form (**RS-TAV**) was found to be higher compared to enantiopure **RR-TAV** and **SS-TAV**. The slow transformation of the **RS-TAV** gel network into crystalline materials indicate that the crystalline nature is predominant in the *meso* form. We also checked the MGC of **TAV**, which is a statistical mixture of **RR-TAV**, **SS-TAV** and **RS-TAV** for comparison and found that the MGC was lower compared to the *meso* and enantiomeric forms. The strong gelation ability of **TAV** may be attributed to the presence of enantiomers (**RR-TAV** & **SS-**

**TAV**) and the *meso* form (**RS-TAV**) in the ternary mixture (**TAV**). Recently, we have shown that the mixed gel of enantiopure *R,R*- and *S,S*-hexyl bis(urea) tagged with methyl phenylalaninate displayed enhanced thermal and mechanical stability compared to enantiopure gels as well as racemic mixture.<sup>30</sup>

**Table 1: Minimum gelator concentration (MGC in wt%)**

Solvent	<b>RR-TAV</b>	<b>SS-TAV</b>	<b>RS-TAV</b>	<b>RR+SS-TAV</b>
Benzene	2.3	2.3	-	2.0
Toluene	3.0	3.0	-	2.0
<i>o</i> -xylene	2.5	2.5	3.5	2.0
<i>m</i> -xylene	2.5	2.5	3.0	1.5
<i>p</i> -xylene	2.5	2.5	3.5	2.0
Mesitylene	1.5	1.5	2.0	1.2
Chlorobenzene	5.5	5.5	-	4.0
EtOH/water (1:1)	4.0	4.0	4.0	3.5

This prompted us to analyze the gelation property of the multi-component gel (**RR+SS**)-**TAV** obtained by mixing equimolar ratio of enantiopure gels **RR-TAV** and **SS-TAV**. The gelation property of the mixture (**RR+SS**)-**TAV** was analyzed in various solvents and the mixture formed gels in various aromatic solvents such as benzene, toluene, *o*-xylene, *m*-xylene, *p*-xylene, mesitylene and chlorobenzene (see Supporting Information, Table S1). The MGC of (**RR+SS**)-**TAV** (Table 1) was lower compared to the corresponding enantiomers and *meso* gels but matched with the MGC of **TAV** mixture, indicating that the presence of enantiomeric mixtures increases the gelation ability in multi-component gels (see Supporting Information, Table S3).

**Table 2: Sol-gel transition temperature ( $T_{gel}$ )**

Solvent	$T_{gel}$ (°C)			
	<b>RR-TAV</b>	<b>SS-TAV</b>	<b>RS-TAV</b>	<b>(RR+SS)-TAV</b>
<i>p</i> -xylene	87.2	87.6	60.0	106.2
<i>m</i> -xylene	90.4	90.2	76.0	102.0
<i>o</i> -xylene	85.2	85.0	63.0	96.3
Mesitylene	100.2	103.1	88.0	116.2
EtOH/water (1:1)	59.1	60.0	52.0	62.5

The thermal stabilities of the gel network were evaluated by gel to solution phase transition temperature test ( $T_{gel}$ ) using "dropping ball" method. The gels were prepared at 4.0 wt% in benzene, toluene, *o*-xylene, *m*-xylene, *p*-xylene, mesitylene and ethanol/water mixture (1:1, v/v). The analysis of  $T_{gel}$  revealed that **RR-TAV** and **SS-TAV** had similar thermal stability (Table 1), which was not surprising because fibres should have identical strength with different optical rotation. The *meso* compound **RS-TAV** displayed significantly low  $T_{gel}$  indicating thermally weaker network compared to enantiomers. Interestingly, the mixture (**RR+SS**)-**TAV** showed consistently high  $T_{gel}$  values in various solvents compared to both enantiopure (**RR-TAV** and **SS-TAV**) and *meso* compound (**RS-TAV**) (Table 2). This clearly indicates that mixing two enantiomers leads to a different self-assembly mode, resulting in enhanced thermal stability. We

also determined  $T_{gel}$  for **TAV** for comparison (see Supporting Information, Table S5), which was found to be similar to the **(RR+SS)-TAV** gel. This corroborates well with fact that the existence of both enantiomers is a key factor and plays an important role in the thermal stability of gel network. The  $T_{gel}$  experiments of the hydrogels performed for enantiomers, *meso*, ternary mixture and the mixed enantiomeric gels did not show drastic differences, which may be attributed to the predominant crystalline nature of these compounds over the gel state in hydrophilic systems. The  $T_{gel}$  experiments of the mixed gels at 4.0 wt% performed by varying the concentration of both **RR-TAV** and **SS-TAV** in *m*-xylene and mesitylene revealed that the thermal stability of the mixed gel depends on the concentration of the enantiomers (see Supporting Information, Table S6).

The comprehensive structural characteristics such as semi solid-like properties and relative strength of the **TAV** gels were evaluated by rheology. Rheological measurements were performed at 4.0 wt% in *m*-xylene to evaluate mechanical properties of **RR-TAV**, **SS-TAV**, **RS-TAV** and **(RR+SS)-TAV**. Initially, a strain sweep was performed to determine the linear viscoelastic region (LVR), where the elastic modulus ( $G'$ ) was independent of the applied strain. The LVR ensured that the gels undergo reversible deformation during the experiments, which will enable us to evaluate the exact structural properties of the gels. The strain sweep measurement revealed that all the four gels displayed constant  $G'$  up to 0.1% of strain (see Supporting Information, Figure S1). The crossover points at which the gel networks collapsed to liquid phase were found at around 0.5-3.0% of strain. Oscillatory frequency sweep experiment was performed between 0.1 to 10.0 Hz at 0.1% of strain. All organogels showed constant elastic ( $G'$ ) and viscous ( $G''$ ) moduli under varying frequency corroborating gel-like behavior (Figure 2).

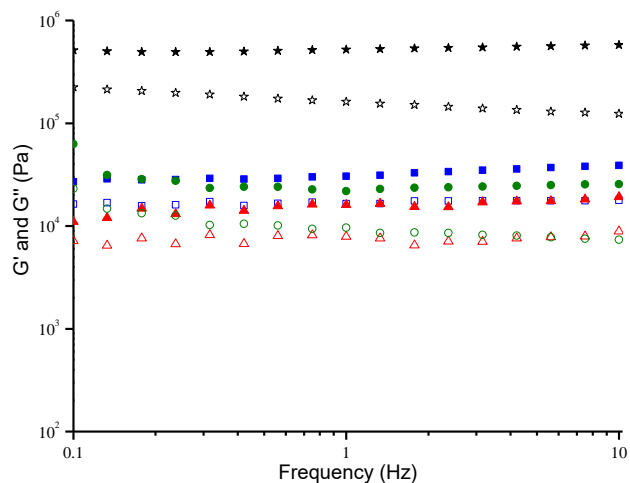


**Figure 2:** Frequency sweep of **TAV** gels (4.0 wt%) in *m*-xylene at 25.0 °C measured at a constant strain of 0.1%. Color codes:  $G'$  **RR-TAV** (■),  $G''$  **RR-TAV** (□),  $G'$  **SS-TAV** (▲),  $G''$  **SS-TAV** (△),  $G'$  **RS-TAV** (●),  $G''$  **RS-TAV** (○),  $G'$  **(RR+SS)-TAV** (★) and  $G''$  **(RR+SS)-TAV** (☆).

The enantiopure and *meso* gels **RR-TAV**, **SS-TAV** and **RS-TAV** displayed similar  $G'$  values in frequency sweep measurements. Interestingly, **(RR+SS)-TAV** gel showed distinctly higher  $G'$  and  $G''$  values compared to the enantiopure

and *meso* gels, which indicate that the mixed gel displayed a relatively rigid network compared to other gels. Rheological measurements were also performed in EtOH/water (1:1, v/v) at 4.0 wt% for all gelators using a heat-cool method (see Supporting Information, Figure S2-S3). The maximum storage modulus values ( $G'$ ) from frequency sweep measurements in EtOH/water indicate that the **RR-TAV** and **SS-TAV** gels were stiffer (>100 kPa) than the other gels (<30 kPa). The mechanical strength of the gels in EtOH/water compared to *m*-xylene gels were different presumably due to the favorable interactions of the enantiomers with hydrogen bonding solvents.

The recent advances in microscopic techniques such as scanning electron microscopy (SEM), transmission electron microscopy (TEM), cryogenic transmission electron microscopy (cryo-TEM), atomic force microscopy (AFM) and confocal laser scanning microscopy (CLSM) enabled researchers to visualize the morphology of self-assembled fibers in multi-component gels.<sup>47-51</sup> Scanning electron microscopy (SEM) is one of the best techniques to visualize the morphology of the fibrous network in LMWGs, which could be used to differentiate self-sorted or co-assembled fibers in multi-component systems. For example, fibers with similar morphologies as individual components were mostly observed in self-sorted systems but it is possible to visualize fibers with different morphologies in co-assembled systems. The organogels were prepared at 4.0 wt% in various solvents and the hydrogel was obtained from EtOH/water (1:1, v/v) at 5.0 wt%. The gels were filtered after 24 hours and dried overnight. The xerogels were placed on a carbon tab and gold coated for 3 minutes. The morphologies of the gels analyzed by SEM revealed typical fibrous morphologies in most of the cases (Figure 3 and see Supporting Information Figure S4-S7).

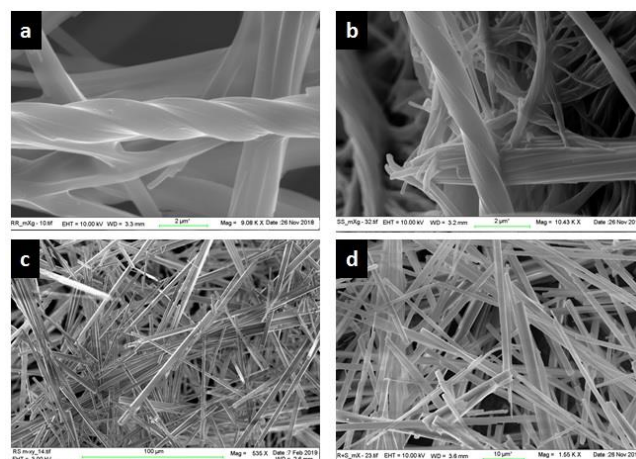


**Figure 3:** SEM images of (a) **RR-**, (b) **SS-**, (c) **RS-** and (d) **(RR+SS)-TAV** xerogels in *m*-xylene at 4.0 wt%.

The enantiopure **RR-TAV** and **SS-TAV** displayed right-handed and left-handed twisted fibers respectively, indicating that the molecular chirality has been translated into the hierarchical aggregates. The diameter of the thin fibers ranged from 250 to 400 nm and the thick fibers were between 600 nm to 1.0  $\mu$ m. The optically inactive *meso* compound **RS-TAV** showed needle like morphology with diameter ranging from 2.0 to 8.0  $\mu$ m. The morphology of mixed **(RR+SS)-TAV** xerogel was different from individual

enantiomers displaying crystalline needle like fibers in all solvents. This indicates the co-assembly of *RR*- and *SS*- compounds in the mixed gel, resulting in the cancellation of opposite helices. The width of the needles ranged from 1.1  $\mu\text{m}$  to 2.4  $\mu\text{m}$  and these needles did not show helicity across all lengths.

The SEM images of the dried hydrogels of all the compounds (5.0 wt%) in 1:1 (v/v) ethanol/water displayed needle and block shaped morphologies (see Supporting Information, Figure S6), which may be attributed to the strong hydrogen bonding interaction between the amide and the polar solvents. The enantiomers displayed twisted needle like morphology and a mixture of needle and block shaped fibers were observed in the *meso* form. The hydrogel of (*RR+SS*)-TAV displayed block shaped morphology indicating that the enantiomers interacted each other to form a co-assembled network, which was confirmed by the absence of self-sorted twisted fibers. The SEM image of the TAV in *m*-xylene and mesitylene indicated a mixture of tape and twisted tape like fibers, which confirms the presence of enantiomers, *meso* and the mixed gels in the ternary mixture (TAV) (see Supporting Information, Figure S7).

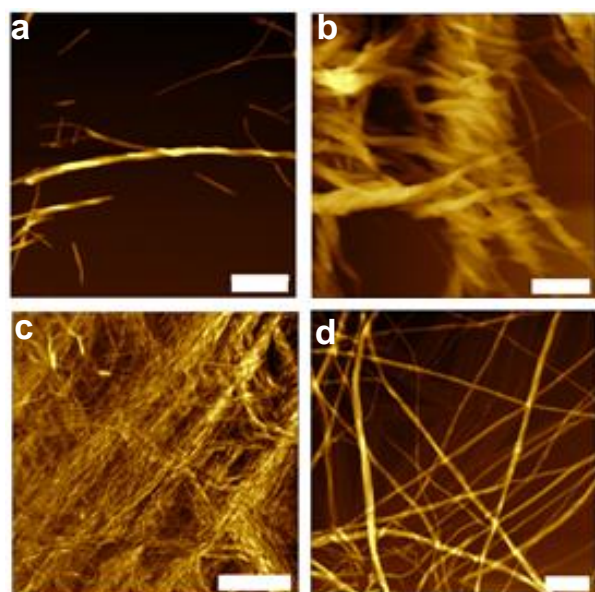


**Figure 4.** AFM images of (a) *RR*-, (b) *SS*-, (c) *RS*- and (d) (*RR+SS*)-TAV gels in EtOH/water (1:1, v/v). Scale bar represents 300 nm in all images except (c), where the scale bar is 1  $\mu\text{m}$ . Samples were spread coated onto freshly cleaved mica at 0.25 wt% apart from (*RR+SS*)-TAV, which was prepared at 0.5 wt%.

To confirm that the fibrous network morphology and handedness observed for all the xerogels from *m*-xylene were also present in 1:1 (v/v) EtOH/water gels, atomic force microscopy (AFM) was undertaken on these samples (Figure 4). As observed in the SEM images, right and left-handed twisted fibers were observed for *RR*- and *SS*-TAV xerogels, respectively. Interestingly, EtOH/water xerogels of *RS*-TAV showed a tightly packed network of smaller fibers which almost appeared braided together, whereas the (*RR+SS*)-TAV xerogel showed long, branched fibers with no evidence of handedness. This is in excellent agreement with the handedness observed in SEM images and suggests a

conservation of specific co-assembly mechanism across different solvent systems. Fibre diameters were largely similar across TAV xerogels of different handedness, with diameters of  $9.7 \pm 2.9$  nm,  $10.8 \pm 1.6$  nm and  $8.4 \pm 2.0$  nm observed for (*RR+SS*)-, *RS*- and *RR*-TAV xerogels respectively. *SS*-TAV xerogels yielded slightly larger fiber diameter of  $19.0 \pm 6.0$  nm, which likely represented a braided arrangement of two individual fibrils, as observed in Figure 4b. The discrepancy between fiber diameters measured through SEM and AFM can be ascribed to a combination of different gelation solvent, coupled with the different concentrations that the measurements were performed. At the higher concentrations (4.0 wt%) used for SEM imaging, it is expected that more aggregation will occur, leading to larger fiber diameters.

Circular dichroism (CD) experiments help to elucidate the structural information of the assembled hierarchical aggregates. CD provides information about the chirality driven self-assembly process, which can be obtained by comparing the CD signals of the solution and gel state. The solution state CD experiments were performed in EtOH at 0.03 wt% to confirm the chirality of these compounds (see Supporting Information, Figure S8). The CD experiments of the gels in aromatic solvents were not possible due to the background absorption of the solvents in CD spectrum. Thus, we have selected hydrogels in 1:1 (v/v) ethanol/water mixture for the CD experiments, which shows absorption cut off at around 190-200 nm. The hydrogels (5.0 wt%) obtained from 1:1 ethanol/water (v/v) mixture was dispersed in a dilute solution of the same solvent mixture to ensure homogeneous dispersion of the fibers in the medium. The CD experiments performed at various concentration revealed that 0.03 wt% was the optimum gelator concentration for these experiments.

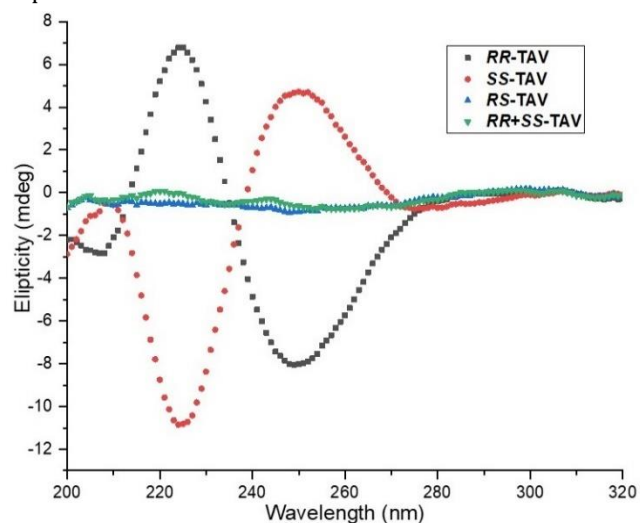


**Figure 5.** CD spectra of *RR*-, *SS*-, *RS*- and (*RR+SS*)-TAV in dispersed gel state measured at 25.0  $^{\circ}\text{C}$ . Gels formed at 5.0 wt% in EtOH/water (1:1 v/v) were diluted with same solvent system to 0.03 wt%.

The CD spectrum of *RR*-TAV showed positive and negative maxima at 225 nm and 250 nm respectively and the overall spectra was found to be mirror image of *SS*-TAV (Figure 5). The peaks at 250 nm may be attributed to the  $\beta$ -sheet like architecture observed in short peptide self-

assembled gels arising from amide hydrogen bonding and  $\pi$ - $\pi$  stacking interactions.<sup>94-96</sup> The *meso* compound **RS-TAV** displayed a linear CD signal and the absence of strong absorption peaks at 225 nm and 250 nm confirmed the cancellation of the optical rotation due to the presence of opposite stereogenic centers. The CD spectrum of the mixed gel of equimolar mixture of **RR-TAV** and **SS-TAV** was similar to the *meso* compound (Figure 5). We have performed the CD at higher water concentration (EtOH/water, 1:4, v/v) for all gels and similar spectra were observed in all cases (see Supporting Information, Figure S9). The experiments were also carried out with different **RR-TAV** and **SS-TAV** ratios in mixed gel. The mixture (**RR-TAV** and **SS-TAV**, 75:25) displayed positive maxima and the mixture (**RR-TAV** and **SS-TAV**, 25:75) displayed negative maxima in both solution (see Supporting Information, Figure S10a) and dispersed gel state (see Supporting Information, Figure S10b) due to the presence of one of the enantiomers in excess.

ATR-FTIR spectroscopy has been used to extract information about the extent of hydrogen bonding in supramolecular gels<sup>43, 46, 97-99</sup> and the difference between N—H stretching peaks in solid-state and gel state will enable elucidation of structural information for the self-assembled hierarchical **TAV** aggregates. The IR spectra recorded in the gel states indicated a slight broadening of the amide band and the N—H stretching peaks were shifted towards lower wavenumber for **RS-TAV** and (**RR+SS**)-**TAV**. The maximum shift (26.0 cm<sup>-1</sup>) was observed for (**RR+SS**)-**TAV** suggesting that the mixed gel network displayed stronger and extended hydrogen bonding compared to other gels (see Supporting Information, Figure S12-S15 & Table S7).

The crystallization experiments were performed in a wide range of solvent or solvent mixtures and single crystals were obtained via slow evaporation over 2-3 days depending upon the solvent used. Analysis of the crystal morphologies revealed that block shaped crystals were obtained for **RR-TAV**, **SS-TAV** and (**RR+SS**)-**TAV** by the vapor phase diffusion of diethyl ether into a toluene solution of the compound and plate shaped crystals were obtained for **RS-TAV**. However, block shaped crystals were obtained for **SS-TAV**, **RS-TAV** and (**RR+SS**)-**TAV** in 1:1 (v/v) aqueous mixture (EtOH/water and 1,4-dioxane/water) whereas **RR-TAV** formed needle shaped crystals. The crystals of **RR-TAV** and **SS-TAV** isolated from different solvents displayed identical structure, which was confirmed by SCXRD and PXRD. The crystallographic details and hydrogen bonding parameters of the compounds are summarized in Table S8 and S9 (see Supporting Information) respectively.

The enantiomers **SS-TAV** and **RR-TAV** crystallized in the chiral  $P2_1$  space group (see Supporting Information, Figure S16 & S17) with three molecules in the asymmetric unit oriented orthogonally to each other. The methyl ester and the aromatic moieties of one of the molecules were disordered in both cases and the structure and hydrogen bonding patterns of these two enantiomers were similar. The nitrogen atom and the oxygen atom of the amide moieties of the gelator displayed N—H $\cdots$ O hydrogen bonding interactions with four molecules to form a hydrogen bonded zig-zag sheet like architecture. In the crystal structure, two zig-zag sheets were oriented perpendicular to each other, which might explain the helical twist in gel fibers of **SS-TAV** and

**RR-TAV** respectively. The *meso* compound **RS-TAV** crystallized in centrosymmetric  $P2_1/c$  space group with an inversion center at the centroid of the phenylene ring (Figure S18) making the molecule optically inactive. The amide moieties displayed similar N—H $\cdots$ O hydrogen bonding interactions as the enantiomers but a 2-D hydrogen bonded sheet like architecture was observed in **RS-TAV**.

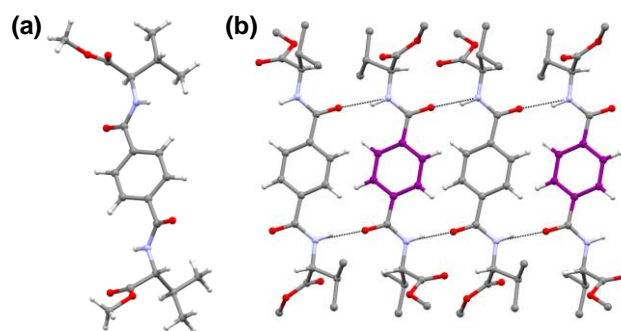


**Figure 6:** Single crystal structure of (**RR+SS**)-**TAV**: (a) asymmetric unit (b) H-bonded 1-D chain showing specific co-assembly; the phenyl carbon atoms of **RR-TAV** and **SS-TAV** are shown in grey and purple color respectively and the hydrogen atoms of the ester and isopropyl groups are omitted for clarity.

The equimolar mixture of the two enantiomers (**RR+SS**)-**TAV** crystallized in centrosymmetric  $P2_1/c$  space group with one enantiomer in the asymmetric unit (Figure 6a), which was related to the other enantiomer via an inversion center. Interestingly, the amide moieties displayed complementary amide hydrogen bonding and the adjacent enantiomer interacted via N—H $\cdots$ O interactions. These interactions resulted in a 1-D hydrogen bonded tape with a sequence of  $-(R-R)-(S-S)-(R-R)-(S-S)-$  confirming the specific co-assembly of two enantiomers (Figure 6b). The 1-D tape interacted with adjacent tapes via various non-bonding interactions, which were oriented perpendicular to each other. The extended 1-D chain-like architecture with co-assembled enantiomers explains the enhanced thermal and mechanical stability of the mixed gels.

The correlation of single crystal structure and the gel network was analyzed by comparing the crystal structure with the powder X-ray diffraction (PXRD) data of the dried gel. The gels obtained from EtOH/water (1:1, v/v, 4.0 wt%) were filtered after 24 hours and dried under a fume hood. The PXRD pattern of the xerogels were compared to the simulated pattern obtained from the crystal structure. PXRD pattern of the xerogel obtained from the mixed (**RR+SS**)-**TAV** gel matched perfectly with the simulated pattern (Figure 7), indicating that the crystal structure truly represents the hierarchical assembly of the xerogel network. This confirms that the translation of specific co-assembly of **RR-TAV** and **SS-TAV** enantiomers from molecular level to mesoscopic xerogel network was achieved. The PXRD pattern of the xerogels of enantiomers (**RR-TAV** and **SS-TAV**) were also found to be similar to the simulated pattern but the peak intensities were lower (Figure S19-S20) presumably due to the low order and less crystallinity of the xerogels compared to the crystalline state.

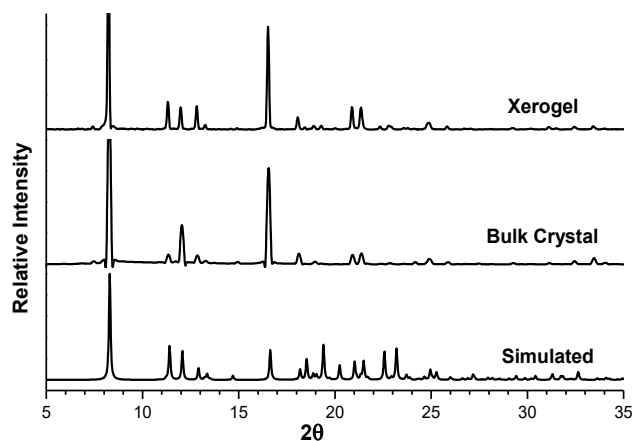


**Figure 7:** Comparison of PXRD pattern of **(RR+SS)-TAV**: simulated, bulk crystals obtained from EtOH/water and xerogel at 4.0 wt% obtained from EtOH/water (1:1, v/v).

The PXRD pattern of **RS-TAV** xerogel matched with the simulated and bulk crystal pattern except a sharp peak at  $8.5^\circ$  ( $2\theta$ ), which may be attributed to the presence of hydrogen bonded solvent molecules in the xerogel (Figure S21). The PXRD pattern of the xerogels and the bulk crystals with the corresponding crystal structures clearly indicate the phase purity of these compounds and proved that the solid-state structure truly represents the hierarchical assembly of the xerogel network. Thus, we have used the combination of single crystal X-ray and powder X-ray diffraction to analyze the self-assembly modes in enantiomeric multi-component gels. Importantly, the results do show unambiguously that **(RR+SS)-TAV** co-assemble in both the solid and the gel state, explaining this mixture has very different stability ( $T_{gel}$ ) and mechanical properties from the individual enantiomers. The correlation of non-bonding interactions in the solid-state structure to the xerogel will add up to the ongoing efforts to identify the key interactions that control the self-assembly process.

## CONCLUSIONS

The self-assembly modes in chiral bis-amide supramolecular gels in all three possible stereoisomeric forms (*R-R*, *S-S* & *R-S*) and mixed enantiomers were studied using X-ray diffraction. The multi-component gel **(RR+SS)-TAV** based on enantiomers was prepared by mixing an equimolar **RR-TAV** and **SS-TAV** and the mixed gel displayed enhanced mechanical and thermal stabilities compared to the enantiomers and the *meso* form. The preservation of chirality of the gel was analyzed by circular dichroism (CD) experiment. The single crystal X-ray diffraction revealed chiral 2-D sheet architecture for both enantiomers, but planar sheet architecture was observed for the *meso* form. The mixed gelator **(RR+SS)-TAV** displayed specific co-assembly of the two enantiomers resulting in a 1-D hydrogen bonded network, which was further supported by scanning electron microscopy (SEM) and atomic force microscopy (AFM) images. The increased thermal and mechanical strength of the mixed gel may be attributed to the enhanced intermolecular forces between the enantiomers leading to specific co-assembly in the mixed gel. The understanding of non-covalent interactions between the individual gelators at molecular level leading to specific co-assembly process will enable

supramolecular chemists to design multi-component systems with tunable properties.

## ASSOCIATED CONTENT

### Supporting Information

Further gelation studies, rheology, SEM images, CD experiments, IR spectra, X-ray crystallography, hydrogen bonding parameters, comparison of powder X-ray pattern and HPLC of RR-, SS-, RS-TAV are supplied as Supporting Information. This material is available free of charge via the Internet at <http://pubs.acs.org>.

## AUTHOR INFORMATION

### Corresponding Author

E-mail: [krishna@hi.is](mailto:krishna@hi.is).

### Notes

The authors declare no competing financial interests.

## ACKNOWLEDGMENT

We thank University of Iceland Research Fund and Science Institute for funding. D.G. thanks the University of Iceland for the Doctoral Research and Teaching Assistantship grant. We thankfully acknowledge Poulami Chakraborty, School of Chemical Sciences, Indian Association for the Cultivation of Science (IACS), Kolkata, India for rheology measurements in *m*-xylene, Dr. Sigurður Sveinn Jónsson, ÍSOR-Iceland for powder X-ray diffraction analysis, Kristinn Ragnar Óskarsson, University of Iceland for CD experiments and Dr. Sigríður Jónsdóttir, University of Iceland for NMR and Mass spectroscopy. We thank Rannís Iceland for infrastructure grants for a single-crystal X-ray diffractometer (150998-0031) and CD spectrometer (171448-0031). P.T. thanks the Australian Research Council for an ARC Centre of Excellence grant (CE140100036) and ARC Discovery Project grant (DP190101892). A.D.M. thanks the National Health and Medical Research Council for a Dementia Development Research Fellowship (APP1106751).

## REFERENCES

- Ball, P., *The Self-Made Tapestry: Pattern Formation in Nature*. Oxford University Press, Inc.: Oxford, U.K, 2001; p 296 pp.
- Lehn, J. M., *Supramolecular Chemistry: Concepts and Perspectives*. Wiley-VCH, Weinheim: Weinheim, Germany, 1995; p 262 pp.
- Comprehensive Supramolecular Chemistry*. Lehn, J. M.; Atwood, J. L.; Davies, J. E. D.; MacNicol, D. D.; Vögtle, F., Eds. Pergamon: Oxford, U.K., 1996; 11 Vols.
- Jean-Marie, L., Perspectives in Chemistry—Steps towards Complex Matter. *Angew. Chem. Int. Ed.* **2013**, *52*, (10), 2836-2850.
- Lehn, J.-M., Constitutional Dynamic Chemistry: Bridge from Supramolecular Chemistry to Adaptive Chemistry. In *Constitutional Dynamic Chemistry*, Barboiu, M., Ed. Springer, Berlin: Heidelberg, 2012; Vol. 322, pp 1-32.
- Jean-Marie, L., Perspectives in Chemistry—Aspects of Adaptive Chemistry and Materials. *Angew. Chem. Int. Ed.* **2015**, *54*, (11), 3276-3289.
- McConnell, A. J.; Wood, C. S.; Neelakandan, P. P.; Nitschke, J. R., Stimuli-Responsive Metal-Ligand Assemblies. *Chem. Rev.* **2015**, *115*, (15), 7729-7793.
- Theato, P.; Sumerlin, B. S.; O'Reilly, R. K.; Epps, I. I. T. H., Stimuli responsive materials. *Chem. Soc. Rev.* **2013**, *42*, (17), 7055-7056.

- (9) Hajime, S.; Itaru, H., Supramolecular Assemblies Responsive to Biomolecules toward Biological Applications. *Chem. Asian J.* **2015**, *10*, (10), 2026-2038.
- (10) Segarra-Maset, M. D.; Nebot, V. J.; Miravet, J. F.; Escuder, B., Control of molecular gelation by chemical stimuli. *Chem. Soc. Rev.* **2013**, *42*, (17), 7086-7098.
- (11) Banerjee, S.; Das, R. K.; Maitra, U., Supramolecular gels 'in action'. *J. Mater. Chem.* **2009**, *19*, (37), 6649-6687.
- (12) Dastidar, P., Supramolecular gelling agents: can they be designed? *Chem. Soc. Rev.* **2008**, *37*, (12), 2699-2715.
- (13) de Loos, M.; Feringa, B. L.; van Esch, J. H., Design and Application of Self-Assembled Low Molecular Weight Hydrogels. *Eur. J. Org. Chem.* **2005**, *2005*, (17), 3615-3631.
- (14) Estroff, L. A.; Hamilton, A. D., Water Gelation by Small Organic Molecules. *Chem. Rev.* **2004**, *104*, (3), 1201-1218.
- (15) George, M.; Weiss, R. G., Molecular Organogels. Soft Matter Comprised of Low-Molecular-Mass Organic Gelators and Organic Liquids†. *Acc. Chem. Res.* **2006**, *39*, (8), 489-497.
- (16) Hirst, A. R.; Escuder, B.; Miravet, J. F.; Smith, D. K., High-Tech Applications of Self-Assembling Supramolecular Nanostructured Gel-Phase Materials: From Regenerative Medicine to Electronic Devices. *Angew. Chem. Int. Ed.* **2008**, *47*, (42), 8002-8018.
- (17) Kumar, D. K.; Steed, J. W., Supramolecular gel phase crystallization: orthogonal self-assembly under non-equilibrium conditions. *Chem. Soc. Rev.* **2014**, *43*, (7), 2080-2088.
- (18) Steed, J. W., Anion-tuned supramolecular gels: a natural evolution from urea supramolecular chemistry. *Chem. Soc. Rev.* **2010**, *39*, (10), 3686-3699.
- (19) Yu, G.; Yan, X.; Han, C.; Huang, F., Characterization of supramolecular gels. *Chem. Soc. Rev.* **2013**, *42*, (16), 6697-6722.
- (20) Buerkle, L. E.; Rowan, S. J., Supramolecular gels formed from multi-component low molecular weight species. *Chem. Soc. Rev.* **2012**, *41*, (18), 6089-6102.
- (21) Edwards, W.; Smith, D. K., Enantioselective Component Selection in Multicomponent Supramolecular Gels. *J. Am. Chem. Soc.* **2014**, *136*, (3), 1116-1124.
- (22) Cross, E. R.; Sproules, S.; Schweins, R.; Draper, E. R.; Adams, D. J., Controlled Tuning of the Properties in Optoelectronic Self-Sorted Gels. *J. Am. Chem. Soc.* **2018**, *140*, (28), 8667-8670.
- (23) Draper, E. R.; Eden, E. G. B.; McDonald, T. O.; Adams, D. J., Spatially resolved multicomponent gels. *Nat. Chem.* **2015**, *7*, 848.
- (24) Colquhoun, C.; Draper, E. R.; Eden, E. G. B.; Cattoz, B. N.; Morris, K. L.; Chen, L.; McDonald, T. O.; Terry, A. E.; Griffiths, P. C.; Serpell, L. C.; Adams, D. J., The effect of self-sorting and co-assembly on the mechanical properties of low molecular weight hydrogels. *Nanoscale* **2014**, *6*, (22), 13719-13725.
- (25) Raeburn, J.; Adams, D. J., Multicomponent low molecular weight gelators. *Chem. Commun.* **2015**, *51*, (25), 5170-5180.
- (26) Swanekamp, R. J.; DiMaio, J. T. M.; Bowerman, C. J.; Nilsson, B. L., Coassembly of Enantiomeric Amphipathic Peptides into Amyloid-Inspired Rippled  $\beta$ -Sheet Fibrils. *J. Am. Chem. Soc.* **2012**, *134*, (12), 5556-5559.
- (27) Edwards, W.; Smith, D., Chiral Assembly Preferences and Directing Effects in Supramolecular Two-Component Organogels. *Gels* **2018**, *4*, (2), 31.
- (28) Brizard, A.; Oda, R.; Huc, I., Chirality Effects in Self-assembled Fibrillar Networks. In *Low Molecular Mass Gelator*, Springer, Berlin: Heidelberg, 2005; pp 167-218.
- (29) Smith, D. K., Lost in translation? Chirality effects in the self-assembly of nanostructured gel-phase materials. *Chem. Soc. Rev.* **2009**, *38*, (3), 684-694.
- (30) Tómasson, D. A.; Ghosh, D.; Kržišnik, Z.; Fasolin, L. H.; Vicente, A. A.; Martin, A. D.; Thordarson, P.; Damodaran, K. K., Enhanced Mechanical and Thermal Strength in Mixed-Enantiomers-Based Supramolecular Gel. *Langmuir* **2018**, *34*, (43), 12957-12967.
- (31) Das, R. K.; Kandanelli, R.; Linnanto, J.; Bose, K.; Maitra, U., Supramolecular Chirality in Organogels: A Detailed Spectroscopic, Morphological, and Rheological Investigation of Gels (and Xerogels) Derived from Alkyl Pyrenyl Urethanes. *Langmuir* **2010**, *26*, (20), 16141-16149.
- (32) Nagy, K. J.; Giano, M. C.; Jin, A.; Pochan, D. J.; Schneider, J. P., Enhanced Mechanical Rigidity of Hydrogels Formed from Enantiomeric Peptide Assemblies. *J. Am. Chem. Soc.* **2011**, *133*, (38), 14975-14977.
- (33) Adhikari, B.; Nanda, J.; Banerjee, A., Multicomponent hydrogels from enantiomeric amino acid derivatives: helical nanofibers, handedness and self-sorting. *Soft Matter* **2011**, *7*, (19), 8913-8922.
- (34) Cicchi, S.; Ghini, G.; Lascialfari, L.; Brandi, A.; Betti, F.; Berti, D.; Baglioni, P.; Di Bari, L.; Pescitelli, G.; Mannini, M.; Caneschi, A., Self-sorting chiral organogels from a long chain carbamate of 1-benzyl-pyrrolidine-3,4-diol. *Soft Matter* **2010**, *6*, (8), 1655-1661.
- (35) Nagy-Smith, K.; Beltramo, P. J.; Moore, E.; Tycko, R.; Furst, E. M.; Schneider, J. P., Molecular, Local, and Network-Level Basis for the Enhanced Stiffness of Hydrogel Networks Formed from Coassembled Racemic Peptides: Predictions from Pauling and Corey. *ACS Cent. Sci.* **2017**, *3*, (6), 586-597.
- (36) Duan, P.; Cao, H.; Zhang, L.; Liu, M., Gelation induced supramolecular chirality: chirality transfer, amplification and application. *Soft Matter* **2014**, *10*, (30), 5428-5448.
- (37) Liu, Z.; Sun, J.; Zhou, Y.; Zhang, Y.; Wu, Y.; Nalluri, S. K. M.; Wang, Y.; Samanta, A.; Mirkin, C. A.; Schatz, G. C.; Stoddart, J. F., Supramolecular Gelation of Rigid Triangular Macrocycles through Rings of Multiple C-H...O Interactions Acting Cooperatively. *J. Org. Chem.* **2016**, *81*, (6), 2581-2588.
- (38) Draper, E. R.; Adams, D. J., How should multicomponent supramolecular gels be characterised? *Chem. Soc. Rev.* **2018**, *47*, (10), 3395-3405.
- (39) Draper, E. R.; Wallace, M.; Schweins, R.; Poole, R. J.; Adams, D. J., Nonlinear Effects in Multicomponent Supramolecular Hydrogels. *Langmuir* **2017**, *33*, (9), 2387-2395.
- (40) Chen, L.; Revel, S.; Morris, K.; Adams, D. J., Energy transfer in self-assembled dipeptide hydrogels. *Chem. Commun.* **2010**, *46*, (24), 4267-4269.
- (41) Felip-León, C.; Díaz-Oltra, S.; Galindo, F.; Miravet, J. F., Chameleonic, Light Harvesting Photonic Gels Based on Orthogonal Molecular Fibrillization. *Chem. Mater.* **2016**, *28*, (21), 7964-7972.
- (42) Draper, E. R.; Lee, J. R.; Wallace, M.; Jäckel, F.; Cowan, A. J.; Adams, D. J., Self-sorted photoconductive xerogels. *Chem. Sci.* **2016**, *7*, (10), 6499-6505.
- (43) Abul-Haija, Y. M.; Roy, S.; Frederix, P. W. J. M.; Javid, N.; Jayawarna, V.; Ulijn, R. V., Biocatalytically Triggered Co-Assembly of Two-Component Core/Shell Nanofibers. *Small* **2014**, *10*, (5), 973-979.
- (44) Sarkar, A.; Dhiman, S.; Chalishazar, A.; George, S. J., Visualization of Stereoselective Supramolecular Polymers by Chirality-Controlled Energy Transfer. *Angew. Chem. Int. Ed.* **2017**, *56*, (44), 13767-13771.
- (45) Sugiyasu, K.; Kawano, S.-i.; Fujita, N.; Shinkai, S., Self-Sorting Organogels with p-n Heterojunction Points. *Chem. Mater.* **2008**, *20*, (9), 2863-2865.
- (46) Xing, P.; Chu, X.; Li, S.; Xin, F.; Ma, M.; Hao, A., Switchable and orthogonal self-assemblies of anisotropic fibers. *New J. Chem.* **2013**, *37*, (12), 3949-3955.
- (47) Moffat, J. R.; Smith, D. K., Controlled self-sorting in the assembly of 'multi-gelator' gels. *Chem. Commun.* **2009**, (3), 316-318.

- (48) Onogi, S.; Shigemitsu, H.; Yoshii, T.; Tanida, T.; Ikeda, M.; Kubota, R.; Hamachi, I., In situ real-time imaging of self-sorted supramolecular nanofibres. *Nat. Chem.* **2016**, *8*, 743.
- (49) Singh, N.; Zhang, K.; Angulo-Pachón, C. A.; Mendes, E.; van Esch, J. H.; Escuder, B., Tandem reactions in self-sorted catalytic molecular hydrogels. *Chem. Sci.* **2016**, *7*, (8), 5568-5572.
- (50) Singh, N.; Maity, C.; Zhang, K.; Angulo-Pachón, C. A.; van Esch, J. H.; Eelkema, R.; Escuder, B., Synthesis of a Double-Network Supramolecular Hydrogel by Having One Network Catalyse the Formation of the Second. *Chem. Eur. J.* **2017**, *23*, (9), 2018-2021.
- (51) An, B.; Wang, X.; Cui, M.; Gui, X.; Mao, X.; Liu, Y.; Li, K.; Chu, C.; Pu, J.; Ren, S.; Wang, Y.; Zhong, G.; Lu, T. K.; Liu, C.; Zhong, C., Diverse Supramolecular Nanofiber Networks Assembled by Functional Low-Complexity Domains. *ACS Nano* **2017**, *11*, (7), 6985-6995.
- (52) Xing, P.; Tham, H. P.; Li, P.; Chen, H.; Xiang, H.; Zhao, Y., Environment-Adaptive Coassembly/Self-Sorting and Stimulus-Responsiveness Transfer Based on Cholesterol Building Blocks. *Adv. Sci.* **2018**, *5*, (1), 1700552.
- (53) Halperin-Sternfeld, M.; Ghosh, M.; Sevostianov, R.; Grigoriants, I.; Adler-Abramovich, L., Molecular co-assembly as a strategy for synergistic improvement of the mechanical properties of hydrogels. *Chem. Commun.* **2017**, *53*, (69), 9586-9589.
- (54) Fichman, G.; Guterman, T.; Adler-Abramovich, L.; Gazit, E., Synergetic functional properties of two-component single amino acid-based hydrogels. *CrystEngComm* **2015**, *17*, (42), 8105-8112.
- (55) Smith, M. M.; Smith, D. K., Self-sorting multi-gelator gels—mixing and ageing effects in thermally addressable supramolecular soft nanomaterials. *Soft Matter* **2011**, *7*, (10), 4856-4860.
- (56) Li, D.; Shi, Y.; Wang, L., Mechanical Reinforcement of Molecular Hydrogel by Co-assembly of Short Peptide-based Gelators with Different Aromatic Capping Groups. *Chin. J. Chem.* **2014**, *32*, (2), 123-127.
- (57) Foster, J. A.; Edkins, R. M.; Cameron, G. J.; Colgin, N.; Fucke, K.; Ridgeway, S.; Crawford, A. G.; Marder, T. B.; Beeby, A.; Cobb, S. L.; Steed, J. W., Blending Gelators to Tune Gel Structure and Probe Anion-Induced Disassembly. *Chem. Eur. J.* **2014**, *20*, (1), 279-291.
- (58) Das, A.; Ghosh, S., A generalized supramolecular strategy for self-sorted assembly between donor and acceptor gelators. *Chem. Commun.* **2011**, *47*, (31), 8922-8924.
- (59) Morris, K. L.; Chen, L.; Raeburn, J.; Sellick, O. R.; Cotanda, P.; Paul, A.; Griffiths, P. C.; King, S. M.; O'Reilly, R. K.; Serpell, L. C.; Adams, D. J., Chemically programmed self-sorting of gelator networks. *Nat. Comm.* **2013**, *4*, 1480.
- (60) Horgan, C. C.; Rodriguez, A. L.; Li, R.; Bruggeman, K. F.; Stupka, N.; Raynes, J. K.; Day, L.; White, J. W.; Williams, R. J.; Nisbet, D. R., Characterisation of minimalist co-assembled fluorenylmethoxycarbonyl self-assembling peptide systems for presentation of multiple bioactive peptides. *Acta Biomater.* **2016**, *38*, 11-22.
- (61) Džolić, Z.; Wolsperger, K.; Žinić, M., Synergic effect in gelation by two-component mixture of chiral gelators. *New J. Chem.* **2006**, *30*, (10), 1411-1419.
- (62) Shigemitsu, H.; Fujisaku, T.; Tanaka, W.; Kubota, R.; Minami, S.; Urayama, K.; Hamachi, I., An adaptive supramolecular hydrogel comprising self-sorting double nanofibre networks. *Nat. Nanotechnol.* **2018**, *13*, (2), 165-172.
- (63) McAulay, K.; Dietrich, B.; Su, H.; Scott, M. T.; Rogers, S.; Al-Hilaly, Y. K.; Cui, H.; Serpell, L. C.; Seddon, Annela M.; Draper, E. R.; Adams, D. J., Using chirality to influence supramolecular gelation. *Chem. Sci.* **2019**, *10*, (33), 7801-7806.
- (64) Kumar, D. K.; Jose, D. A.; Das, A.; Dastidar, P., First snapshot of a nonpolymeric hydrogelator interacting with its gelling solvents. *Chem. Commun.* **2005**, (32), 4059-4061.
- (65) Abraham, S.; Lan, Y.; Lam, R. S. H.; Grahame, D. A. S.; Kim, J. J. H.; Weiss, R. G.; Rogers, M. A., Influence of Positional Isomers on the Macroscale and Nanoscale Architectures of Aggregates of Racemic Hydroxyoctadecanoic Acids in Their Molecular Gel, Dispersion, and Solid States. *Langmuir* **2012**, *28*, (11), 4955-4964.
- (66) Xu, Y.; Kang, C.; Chen, Y.; Bian, Z.; Qiu, X.; Gao, L.; Meng, Q., In Situ Gel-to-Crystal Transition and Synthesis of Metal Nanoparticles Obtained by Fluorination of a Cyclic  $\beta$ -Aminoalcohol Gelator. *Chem. Eur. J.* **2012**, *18*, (52), 16955-16961.
- (67) Wang, Y.; Tang, L.; Yu, J., Investigation of Spontaneous Transition from Low-Molecular-Weight Hydrogel into Macroscopic Crystals. *Cryst. Growth Des.* **2008**, *8*, (3), 884-889.
- (68) Braga, D.; d'Agostino, S.; D'Amen, E.; Grepioni, F., Polymorphs from supramolecular gels: four crystal forms of the same silver(i) supergelator crystallized directly from its gels. *Chem. Commun.* **2011**, *47*, (18), 5154-5156.
- (69) Byrne, P.; Lloyd, G. O.; Applegarth, L.; Anderson, K. M.; Clarke, N.; Steed, J. W., Metal-induced gelation in dipyriddy ureas. *New J. Chem.* **2010**, *34*, (10), 2261-2274.
- (70) Dastidar, P.; Roy, R.; Parveen, R.; Sarkar, K., Supramolecular Synthon Approach in Designing Molecular Gels for Advanced Therapeutics. *Adv. Therap.* **2019**, *2*, (1), 1800061.
- (71) Kumar, D. K.; Jose, D. A.; Dastidar, P.; Das, A., Nonpolymeric Hydrogelator Derived from N-(4-Pyridyl)isonicotinamide. *Langmuir* **2004**, *20*, (24), 10413-10418.
- (72) Engstrom, J. R.; Savyasachi, A. J.; Parhizkar, M.; Sutti, A.; Hawes, C. S.; White, J. M.; Gunnlaugsson, T.; Pfeffer, F. M., Norbornene chaotropic salts as low molecular mass ionic organogelators (LMIOGs). *Chem. Sci.* **2018**, *9*, (23), 5233-5241.
- (73) Ghosh, D.; Lebedyć, I.; Yufit, D. S.; Damodaran, K. K.; Steed, J. W., Selective gelation of N-(4-pyridyl)nicotinamide by copper(ii) salts. *CrystEngComm* **2015**, *17*, (42), 8130-8138.
- (74) Sahoo, P.; Kumar, D. K.; Raghavan, S. R.; Dastidar, P., Supramolecular Synthons in Designing Low Molecular Mass Gelling Agents: L-Amino Acid Methyl Ester Cinnamate Salts and their Anti-Solvent-Induced Instant Gelation. *Chem. Asian J.* **2011**, *6*, (4), 1038-1047.
- (75) Anantharaj, S.; Jayakannan, M., Polymers from Amino acids: Development of Dual Ester-Urethane Melt Condensation Approach and Mechanistic Aspects. *Biomacromolecules* **2012**, *13*, (8), 2446-2455.
- (76) Karmakar, A.; Oliver, C. L.; Platero-Prats, A. E.; Laurila, E.; Öhrström, L., Crystal structures and hydrogen bond analysis of five amino acid conjugates of terephthalic and benzene-1,2,3-tricarboxylic acids. *CrystEngComm* **2014**, *16*, (35), 8243-8251.
- (77) Li, K.; Liang, S.; Lu, Y.; Wang, Q., Synthesis of Telechelic Fluoropolymers with Well-Defined Functional End Groups for Cross-Linked Networks and Nanocomposites. *Macromolecules* **2007**, *40*, (12), 4121-4123.
- (78) Dolomanov, O. V.; Bourhis, L. J.; Gildea, R. J.; Howard, J. A. K.; Puschmann, H., OLEX2: a complete structure solution, refinement and analysis program. *J. Appl. Crystallogr.* **2009**, *42*, (2), 339-341.
- (79) Sheldrick, G. M., Crystal structure refinement with SHELXL. *Acta Crystallogr. Sect. C* **2015**, *71*, (Pt 1), 3-8.
- (80) Babu, S. S.; Praveen, V. K.; Ajayaghosh, A., Functional  $\pi$ -Gelators and Their Applications. *Chem. Rev.* **2014**, *114*, (4), 1973-2129.

- (81) Leiras, S.; Freire, F.; Quiñoá, E.; Riguera, R., Reversible assembly of enantiomeric helical polymers: from fibers to gels. *Chem. Sci.* **2015**, *6*, (1), 246-253.
- (82) Zhang, L.; Jin, Q.; Liu, M., Enantioselective Recognition by Chiral Supramolecular Gels. *Chem. Asian J.* **2016**, *11*, (19), 2642-2649.
- (83) Hanabusa, K.; Yamada, M.; Kimura, M.; Shirai, H., Prominent Gelation and Chiral Aggregation of Alkylamides Derived from trans-1,2-Diaminocyclohexane. *Angew. Chem. Int. Ed.* **1996**, *35*, (17), 1949-1951.
- (84) Li, P.; Yin, Z.; Dou, X.-Q.; Zhou, G.; Feng, C.-L., Convenient Three-Dimensional Cell Culture in Supramolecular Hydrogels. *ACS Appl. Mater.* **2014**, *6*, (10), 7948-7952.
- (85) Liu, G.-F.; Ji, W.; Feng, C.-L., Installing Logic Gates to Multiresponsive Supramolecular Hydrogel Co-assembled from Phenylalanine Amphiphile and Bis(pyridinyl) Derivative. *Langmuir* **2015**, *31*, (25), 7122-7128.
- (86) Wang, F.; Qin, M.; Peng, T.; Tang, X.; Yinme Dang-i, A.; Feng, C., Modulating Supramolecular Chirality in Alanine Derived Assemblies by Multiple External Stimuli. *Langmuir* **2018**, *34*, (26), 7869-7876.
- (87) Dou, X.; Li, P.; Zhang, D.; Feng, C.-L., C<sub>2</sub>-symmetric benzene-based hydrogels with unique layered structures for controllable organic dye adsorption. *Soft Matter* **2012**, *8*, (11), 3231-3238.
- (88) Yu, S.-L.; Dou, X.-Q.; Qu, D.-H.; Feng, C.-L., C<sub>2</sub>-symmetric benzene-based organogels: A rationally designed LMOG and its application in marine oil spill. *J. Mol. Liq.* **2014**, *190*, 94-98.
- (89) Cai, W.; Feng, C.; Ma, X.; Chen, M.; Liu, J., C<sub>2</sub>-Symmetric Benzene-based Low Molecular Weight Hydrogel Modified Electrode for Highly Sensitive Detection of Copper Ions. *Electrochim. Acta* **2015**, *169*, 424-432.
- (90) Yu, Y.; Wang, Y.; Feng, C., Hybrid hydrogels assembled from phenylalanine derivatives and agarose with enhanced mechanical strength. *Chem. Res. Chinese U.* **2016**, *32*, (5), 872-876.
- (91) Suzuki, M.; Hanabusa, K., l-Lysine-based low-molecular-weight gelators. *Chem. Soc. Rev.* **2009**, *38*, (4), 967-975.
- (92) Allix, F.; Curcio, P.; Pham, Q. N.; Pickaert, G.; Jamart-Grégoire, B., Evidence of Intercolumnar  $\pi$ - $\pi$  Stacking Interactions in Amino-Acid-Based Low-Molecular-Weight Organogels. *Langmuir* **2010**, *26*, (22), 16818-16827.
- (93) Dirany, M.; Ayzac, V.; Isare, B.; Raynal, M.; Bouteiller, L., Structural Control of Bisurea-Based Supramolecular Polymers: Influence of an Ester Moiety. *Langmuir* **2015**, *31*, (42), 11443-11451.
- (94) Gupta, M.; Bagaria, A.; Mishra, A.; Mathur, P.; Basu, A.; Ramakumar, S.; Chauhan, V. S., Self-Assembly of a Dipeptide-Containing Conformationally Restricted Dehydrophenylalanine Residue to Form Ordered Nanotubes. *Adv. Mater.* **2007**, *19*, (6), 858-861.
- (95) Qin, S.-Y.; Pei, Y.; Liu, X.-J.; Zhuo, R.-X.; Zhang, X.-Z., Hierarchical self-assembly of a  $\beta$ -amyloid peptide derivative. *J. Mater. Chem. B* **2013**, *1*, (5), 668-675.
- (96) Shin, S.; Lim, S.; Kim, Y.; Kim, T.; Choi, T.-L.; Lee, M., Supramolecular Switching between Flat Sheets and Helical Tubules Triggered by Coordination Interaction. *J. Am. Chem. Soc.* **2013**, *135*, (6), 2156-2159.
- (97) Fornaro, T.; Burini, D.; Biczysko, M.; Barone, V., Hydrogen-Bonding Effects on Infrared Spectra from Anharmonic Computations: Uracil-Water Complexes and Uracil Dimers. *J. Phys. Chem. A* **2015**, *119*, (18), 4224-4236.
- (98) Nebot, V. J.; Armengol, J.; Smets, J.; Prieto, S. F.; Escuder, B.; Miravet, J. F., Molecular Hydrogels from Bolaform Amino Acid Derivatives: A Structure-Properties Study Based on the Thermodynamics of Gel Solubilization. *Chem. Eur. J.* **2012**, *18*, (13), 4063-4072.
- (99) Tang, Y.-T.; Dou, X.-Q.; Ji, Z.-A.; Li, P.; Zhu, S.-M.; Gu, J.-J.; Feng, C.-L.; Zhang, D., C<sub>2</sub>-symmetric cyclohexane-based hydrogels: A rational designed LMWG and its application in dye scavenging. *J. Mol. Liq.* **2013**, *177*, 167-171.

For Table of Contents Only

---

